

**Controlling Phase Separated Domains in UV-Curable Formulations with OH-Functionalized Prepolymers**

Journal:	<i>Polymer Chemistry</i>
Manuscript ID	PY-ART-02-2022-000159.R1
Article Type:	Paper
Date Submitted by the Author:	17-Apr-2022
Complete List of Authors:	Hasa, Erion; University of Iowa, Chemical and Biochemical Engineering Lee, Taiyeon; Covestro, Additive Manufacturing Guymon, C.; University of Iowa, Chemical and Biochemical Engineering

# **Controlling Phase Separated Domains in UV-Curable Formulations with OH-Functionalized Prepolymers**

Erion Hasa\*<sup>1</sup>, Tai Yeon Lee<sup>2</sup> and C. Allan Guymon\*\*<sup>1</sup>

<sup>1</sup>Department of Chemical & Biochemical Engineering, University of Iowa, Iowa City, IA 52242,  
United States

<sup>2</sup>Covestro Additive Manufacturing, 1122 Saint Charles St, Elgin, IL 60120, United States

\*Erion Hasa

Covestro Additive Manufacturing

1122 Saint Charles St, Elgin, IL 60120, United States

Phone: 319-237-5475

E-mail: [erion.hasa@covestro.com](mailto:erion.hasa@covestro.com)

\*\*Corresponding author

C. Allan Guymon

Department of Chemical & Biochemical Engineering, University of Iowa

Phone: 319-335-5015; Fax : 319-335-1415

E-mail: [allan-guymon@uiowa.edu](mailto:allan-guymon@uiowa.edu)

## Abstract

Modification of photocurable radical systems with higher molecular weight prepolymers enables access to a wide array of polymer structures and properties. Chemical structure design of these prepolymers may lead to photopolymerization-induced phase separation in such which the domain size and distribution as well as the interactions between prepolymers and the polymer network may be controlled. In this work, we use a controlled radical polymerization technique to synthesize prepolymers composed of butyl acrylate (BA) and hydroxyethyl acrylate in order to create hydroxyl (OH) pendant groups either at the ends or randomly distributed along the predominantly BA chain. Modulating the OH group placement and prepolymers molecular weight has a significant impact on polymer structure and properties of cross-linked acrylate systems. Specifically, photopolymerization of tetraethylene glycol diacrylate (TTGDA) with prepolymers leads to a variety of distinct phase-separated morphologies and phase distributions. These morphological changes along with the incorporation of linear low  $T_g$  prepolymers within the glassy acrylate network increase polymer elongation at break up to a 9-fold while slightly reducing Young's modulus. Consequently, these systems demonstrate a significant increase in tensile toughness at different temperatures due to formation of multiple domains. Additionally, incorporation of prepolymers into a 3D printing model acrylate formulation leads to objects with more than 500% increase in impact strength. This study shows that placement of OH groups at the ends or throughout the BA backbone enables various phase-separated morphologies for photocurable radical systems, generating polymers with enhanced elongation at break, tensile toughness, and impact strength.

Keywords: Photopolymerization, phase separation, radical systems, OH-functionalized prepolymers, enhanced toughness

## Introduction

The formation of materials with nano/micro-structured domains has enabled a variety of enhanced properties including toughness, strength, and ion conductivity.<sup>1-3</sup> Previous studies have shown that polymer morphology and properties can be controlled using methods including photo-induced phase separation, incorporating nanofillers, and utilizing block copolymers.<sup>4-8</sup> For example, photocuring systems with acrylates and oxetanes at a specific monomer ratio resulted in various phase-separated domains that enable better control over the thermomechanical properties (e.g. glass transition temperature ( $T_g$ ), elongation at break, and toughness).<sup>4,5</sup> Others have shown that the incorporation of nanofillers (e.g. graphene oxide and calcium carbonate) can enhance polymer properties. For example, polymer composites with significantly increased  $T_g$ , modulus, and yield stress were obtained with increased filler dispersion and enhanced filler/matrix interaction.<sup>9,10</sup>

Additionally, manipulating the architecture of oligomers has enabled better control of reaction kinetics, polymer morphology, and mechanical properties.<sup>11</sup> For example, thermoplastic triblock (ABA) oligomers with soft and hard domains induce macrophase separation. With lower concentration of the hard domain, morphologies with spherical glassy domains surrounded by a more elastic network were formed leading to increased elongation at break. On the other hand, increasing hard domain concentration enabled formation of co-continuous glassy/rubbery domains resulting in enhanced Young's modulus.<sup>12</sup> Other studies have shown that changing the oligomer architecture (e.g. triblock, random, and V-shaped gradient) can lead to significantly different phase-separated morphologies and properties.<sup>13</sup> For example, block and gradient oligomers

demonstrated co-continuous domains that enable significant increases in elongation at break while random oligomers formed single-domain structures with improved elastic modulus.

Furthermore, incorporation of photopolymerizable urethane-based reactive oligomers has been used to control reaction rate and double bond conversion, and can lead to polymer networks with significantly higher thermal stability, water absorption, and strength.<sup>14</sup> Recent work has also shown that photopolymerization of cationic resins modified with epoxy-functionalized prepolymers of varying architecture results in the formation of different nano/micro-structured polymers with controlled cross-link density and  $T_g$  accompanied by increased elongation at break. These changes were associated with the prepolymer molecular weight and concentration that change prepolymer-network interactions.<sup>5</sup> Consequently, it is reasonable to assume that modifying the molecular weight, functionality, backbone chain, and pendant groups in custom-synthesized prepolymers could lead to controlled polymerization kinetics, polymer morphology, and thermomechanical properties.<sup>15-17</sup>

This research examines the incorporation of custom-synthesized polymers into radically-photopolymerized diacrylate systems to influence polymer structure development and interactions between the acrylate cross-linked network and the linear prepolymers. Specifically, controlled radical polymerization was used to synthesize prepolymers with butyl acrylate (BA) as the main chain (hydrophobic segment) and hydroxyethyl acrylate (HEA) to provide OH pendant groups (hydrophilic segment). The OH groups are either located at both ends or randomly distributed along the prepolymer chain. The effect of this placement on photo-induced phase separation and thermomechanical properties at different temperatures was determined. We hypothesize that

photopolymerization of hydrophilic diacrylate systems modified with OH-functionalized prepolymers will induce different phase-separated morphologies with changing OH placement and prepolymer chain length. It is expected that the molecular weight of prepolymers and the resultant formulation viscosity will influence reaction kinetics and thus domain development during photopolymerization. Consequently, reaction rate as a function of conversion was determined for all prepolymer-modified systems using photo-differential scanning calorimetry. Additionally, the placement of OH groups will likely influence hydrogen bonding interactions between the linear prepolymers and cross-linked acrylate network, impacting overall morphological development and thermomechanical properties. To investigate the variations in polymer morphologies imparted from the different prepolymers, atomic force microscopy was used. The formation of phase-separated domains was confirmed by the presence of multiple  $\tan(\delta)$  peaks obtained using dynamic mechanical analysis (DMA). In addition, DMA was utilized to investigate other polymer properties including stress-strain behavior, storage modulus, and tensile toughness at room and increased temperatures. Lastly, the effect of prepolymer addition into a commercially available acrylate formulation on the performance of 3D printed objects was investigated via impact strength. This research shows that photo-induced phase separation in acrylate systems modified with OH-functionalized prepolymers can be used to fabricate polymers with distinct nano/micro-structured domains, contributing to improved toughness and impact strength. The incorporation of prepolymers into a commercially available resin also indicates that these materials can be used for enhanced mechanical properties in 3D printing applications.

## **Experimental Section**

### **Materials**

Tetraethylene glycol diacrylate (TTGDA) and the reactive urethane diacrylate oligomer (CN9002) were provided by Sartomer. Butyl acrylate (BA), 2-hydroxyethyl acrylate (HEA), and dibenzyl trithiocarbonate (DBTTC) were obtained from Sigma Aldrich. A model acrylate formulation (PR48) appropriate for 3D printing was provided by Colorado Photopolymer Solutions.<sup>18</sup> 2,2-dimethoxy-1,2-diphenylethan-1-one (DMPA, Ciba Specialty Chemicals) was used as the radical photoinitiator for thin film systems while diphenyl(2,4,6-trimethylbenzoyl)phosphine oxide (TPO) was used for 3D printing constructs. All chemicals were used as received.

## Synthesis

Reversible addition-fragmentation chain transfer (RAFT) polymerization is a versatile method to synthesize prepolymers with controlled architecture.<sup>6,19</sup> Production of prepolymers via this method using common RAFT agents such as trithiocarbonates allows polymer network re-arrangements during UV illumination because the RAFT agents remain reactive.<sup>20</sup> In this study, DBTTC raft agent was used to prepare prepolymers with different average number molecular weight ( $M_n$ ) and architecture (Figure 1). For the synthesis of prepolymers with OH pendant groups, a similar procedure from that described by Scholte et al. was followed.<sup>6</sup> To place OH groups on the end sides of a BA backbone, a formulation composed of 4:4:1 (w/w/w) BA/ethyl acetate/HEA was introduced into a round bottom flask and heated to a temperature of approximately 100 °C. A second feed with only BA diluted to 50 wt% with ethyl acetate was then added to the reactor. Conversely, a single mixture composed of 4:4:1 (w/w/w) BA/ethyl acetate/HEA was added to the reactor and allowed to polymerize at the same temperature in order to generate prepolymers with OH groups placed randomly on the BA backbone.

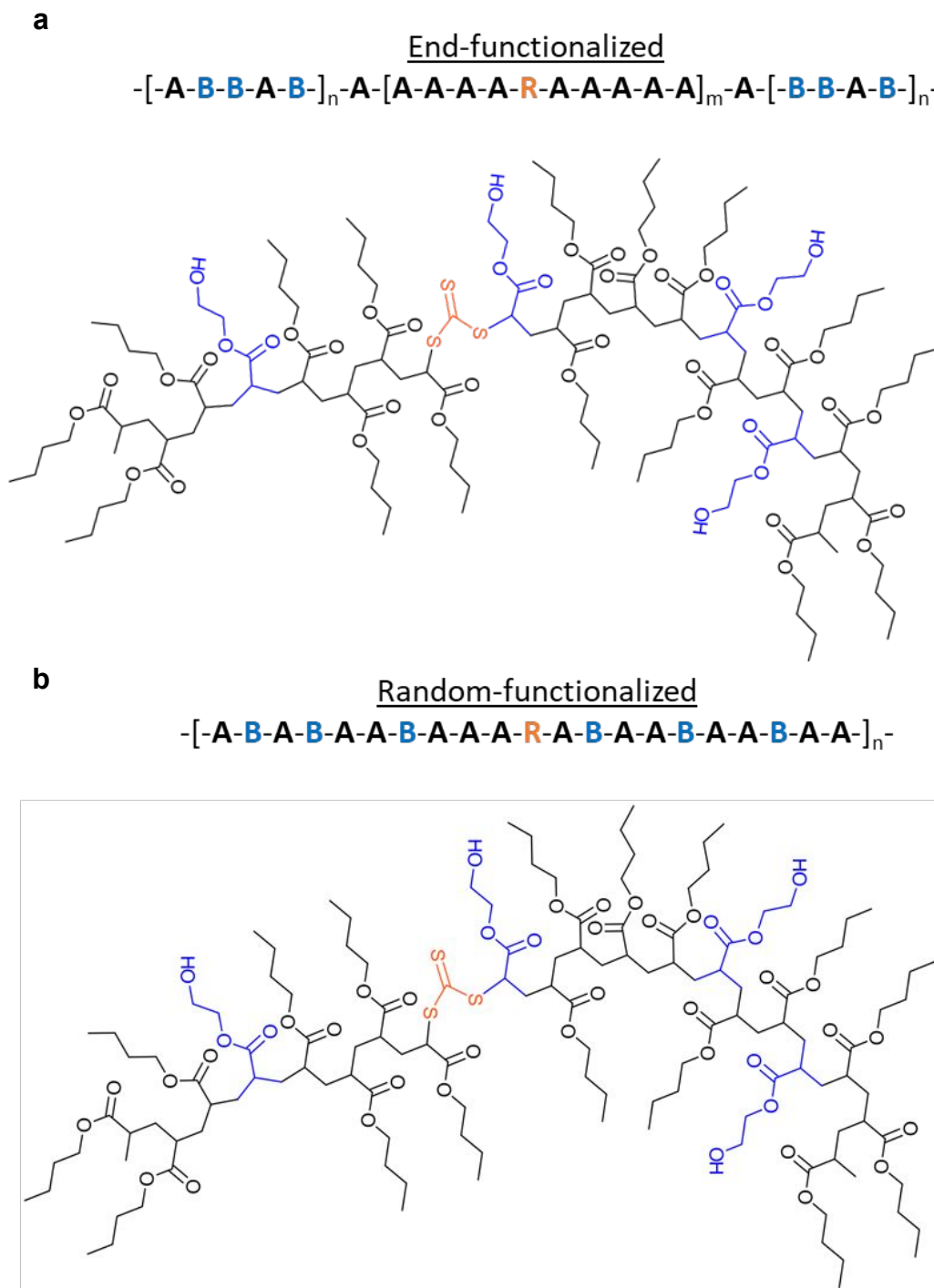


**Figure 1.** Representation of prepolymer structures with the HEA (**B**) located the a) end and b) randomly distributed on the BA (**A**) chain. Both prepolymers are formed using a 4:1 (w/w) BA/HEA ratio and a RAFT agent (**R**).



The  $M_n$  of prepolymers was controlled by changing the amount of azobisisobutyronitrile (AIBN) thermal initiator with higher concentrations leading to lower  $M_n$ . In addition, a ratio of 10:1 (w/w) RAFT/AIBN was maintained for all mixtures. Each prepolymer synthesis was conducted under a nitrogen environment for the entire polymerization. Once the desired  $M_n$  was achieved, as measured by gel permeation chromatography (GPC), the reaction was quenched by adding a small amount of AIBN and removing the heat. All unreacted monomer and solvent were removed using a rotary evaporator for 1 h at approximately 60 °C.

**Table 1.** Properties of OH-modified prepolymers used in this study.

Sample	OH placement	$M_n$ (g/mol)	PDI
<b>E15K</b>	End	15700	1.20
<b>E30K</b>	End	28500	1.10
<b>E50K</b>	End	48700	1.25
<b>R15K</b>	Random	16600	1.30
<b>R30K</b>	Random	30400	1.15
<b>R50K</b>	Random	48700	1.10

Liquid formulations were prepared using a ratio of 2:1 (w/w) TTGDA/prepolymer and 0.5 wt % DMPA. Samples were mixed for about 5 minutes until the photoinitiator was fully dissolved. It is important to mention that all samples using this monomer/prepolymer ratio were optically clear and stable for several days, indicating that these systems are compatible and do not phase separate prior to photopolymerization. Samples were photopolymerized at 10 mW/cm<sup>2</sup> for 10 min at room temperature (approximately 23 °C) using a high-pressure mercury arc lamp (Omnigore S1500 spot

cure system) equipped with a 320-390 nm bandpass filter unless otherwise stated. For 3D printing experiments, systems with 4:1 (w/w) PR48/prepolymer were used. PR48 was selected instead of TTGDA because of its suitability for DLP 3D printing and robust mechanical properties.<sup>21</sup> In this case, a 405 nm LED light source was used to cure each layer of approximately 50  $\mu\text{m}$  thick at 20  $\text{mW}/\text{cm}^2$  for 3.5 s.

## Methods

Photopolymerization kinetics were examined using a Perkin Elmer Diamond differential scanning calorimeter (DSC). To examine the heat flow during polymerization, approximately 2.5 mg samples were placed into a DSC pan and photocured at 10  $\text{mW}/\text{cm}^2$  using a medium-pressure mercury arc lamp as a UV light source. Polymerization rates were normalized by the initial TTGDA concentration and determined using the evolved heat of polymerization per acrylate group according to Equation 1

$$R_p = \frac{Q \times MW}{\Delta H \times n \times m} \quad (1)$$

where  $R_p$  is the normalized rate of polymerization,  $Q$  is the heat flow as measured by the DSC,  $MW$  is the molecular weight of the monomer,  $\Delta H$  is the enthalpy of reaction for an acrylate functional group (20.6 kcal/mol),<sup>22</sup>  $n$  is the number of reactive groups per monomer molecule, and  $m$  is the mass of monomer in the sample.

Atomic force microscopy (AFM; Asylum Research Molecular Force Probe 3D Classic) was used to investigate polymer surface morphology. Phase images were obtained in tapping mode at a rate of 1 Hz and were analyzed with Igor software. A small amount of each monomer formulation was injected between two glass slides separated with 0.25 mm thick tape spacers. Thereafter, samples

were photopolymerized at  $10 \text{ mW/cm}^2$  for 10 min. One glass slide was removed to allow examination of the surface morphology.

Dynamic mechanical analysis (DMA; Q800 DMA TA Instruments) was used to investigate thermomechanical properties such as glass transition temperature, storage modulus, and stress as a function of strain. Small amounts of liquid mixture were photopolymerized at  $10 \text{ mW/cm}^2$  between two glass slides separated by 0.25 mm thickness adhesive tape. The resulting polymer was then cut into rectangle shapes with dimensions of approximately  $8 \times 6 \times 0.25 \text{ mm}$  (L  $\times$  W  $\times$  T). DMA tensile mode was used under constant strain at a frequency of 1 Hz and a heating rate of  $4 \text{ }^\circ\text{C/min}$  to observe the  $\tan(\delta)$  behavior and obtain information regarding the glass transition temperature(s) and storage modulus. Additionally, stress as a function of strain was evaluated using DMA tensile mode with a force rate of  $1.0 \text{ N/min}$ . The initial slope and the area under stress and strain curves until break were calculated to estimate Young's modulus and toughness, respectively.

The impact strength of 3D printed parts composed of PR48 and different prepolymers was determined using a pendulum impact tester HIT5.5P (Zwick Roell). All tests were conducted using an Izod fixture at room temperature. The izod parts were fabricated using an Autodesk Ember digital light projection (DLP) 3D printer equipped with a 405 nm LED light source that produces approximately  $20 \text{ mW/cm}^2$ . More information regarding the operation of the 3D printer can be found elsewhere.<sup>21</sup> The dimensions of each specimen were approximately  $40 \times 10 \times 7 \text{ mm}$  (L  $\times$  W  $\times$  T). In addition, all specimen were designed with a notch (2 mm/ $45^\circ$  radius) to better examine the resistance to sudden impact.

The  $M_n$  and polydispersity index (PDI) of each prepolymer were obtained using multi-angle static light scattering (MALS; Dawn Heleos II) in conjunction with a gas permeation chromatography (GPC). Before testing the  $M_n$  of prepolymers, the instrument was calibrated using polystyrene standards. A small amount (20  $\mu\text{L}$ ) of prepolymer diluted in tetrahydrofuran was then injected in the GPC-MALS system and allowed to pass through a PLgel Mixed-D column at a flow rate of 0.5 mL/min. The  $M_n$  and PDI were measured by comparing the elution time of prepolymers with that of the polystyrene standards.

## Results and Discussion

### *Reaction Rate and Conversion*

Photopolymerization enables fast network formation which, in turn, leads to dramatic changes in several characteristics including viscosity, cross-linking, vitrification, and glass transition temperature.<sup>23</sup> Thus, basic photopolymerization kinetics directly impact polymer network and property evolution. Among many parameters, polymerization kinetics depend on monomer/prepolymer molecular weight and reactivity, light intensity, and polymerization temperature.<sup>4,6,24</sup> Typically, the double bond conversion of (meth)acrylates increases with the lower molecular weight prepolymers due to enhanced diffusion of monomer reactive species and decreased termination rate. When, however, prepolymers with much higher molecular weight are used, the opposite effect may occur resulting in lower double bond conversion due to high viscosity and very limited diffusion.<sup>15,17</sup> In this study, we incorporate OH-functionalized prepolymers with varying molecular weight into a tetraethylene glycol diacrylate (TTGDA) system. Due to differences in molecular weight of prepolymers and the placement of OH groups on the BA

backbone, both reaction rate and final acrylate conversion may change, affecting ultimate polymer properties. Figure 2 shows the reaction rate as a function of conversion for the control TTGDA system and for prepolymer containing systems during photopolymerization at 10 mW/cm<sup>2</sup>. The system with neat TTGDA reaches the maximum rate relatively quickly at around 25% double bond conversion, with a final conversion of nearly 70%. This behavior is typical for highly cross-linked systems which reach limited conversions due to early gelation and vitrification.<sup>25</sup>

The incorporation of prepolymers impacts both the maximum rate and final conversion. The addition of either end or random-functionalized prepolymers leads to increased conversion and the maximum rate. Specifically, the final acrylate conversion appears to increase from around 70% for the neat TTGDA to 90-95% depending on the prepolymer type and  $M_n$ . Although the prepolymer addition helps to increase final conversion, this increase occurs to a lesser extent (about 80%) in TTGDA/E50k systems likely due to more limited diffusion of polymer radicals and self-association of E50k prepolymer. Interestingly, the reaction rate and conversion of TTGDA/R50k system does not have the same behavior with that of TTGDA/E50k system. This behavior could be due to more uniform OH group placement along the prepolymer chain, allowing more distributed hydrogen bonding interactions between R50k prepolymers and the TTGDA network. The observed changes in reaction kinetics of TTGDA systems due to prepolymer addition could be associated with the enhanced mobility of reactive species.<sup>15,26</sup> Additionally, previous studies have shown that the presence of hydroxyl groups form a variety of hydrogen bonds which may further accelerate overall polymerization rate and conversion of the acrylate functional groups.<sup>27-</sup>

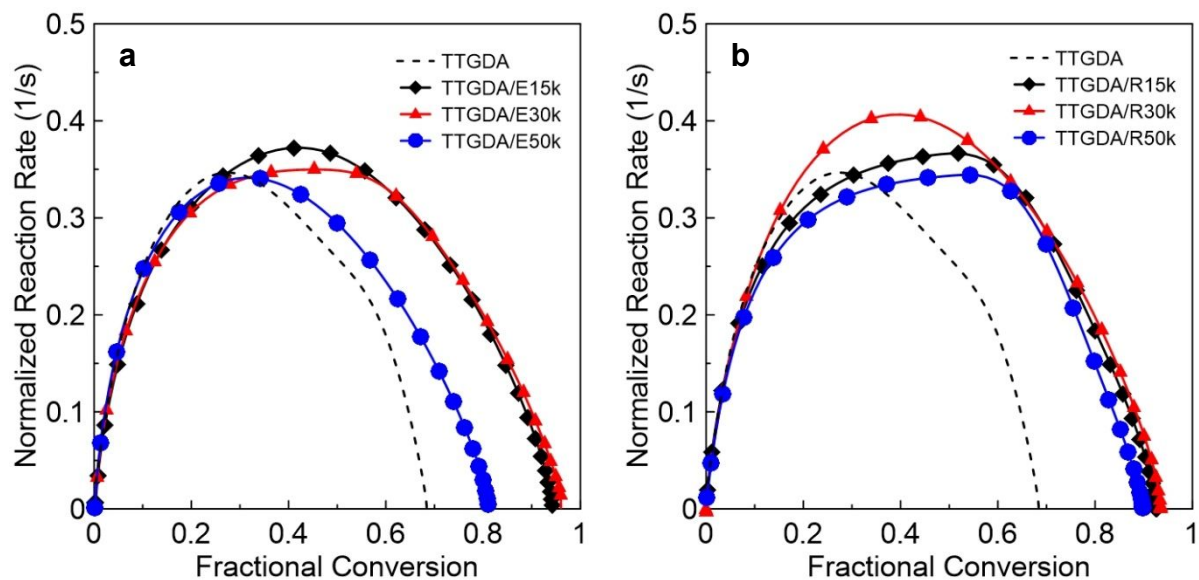


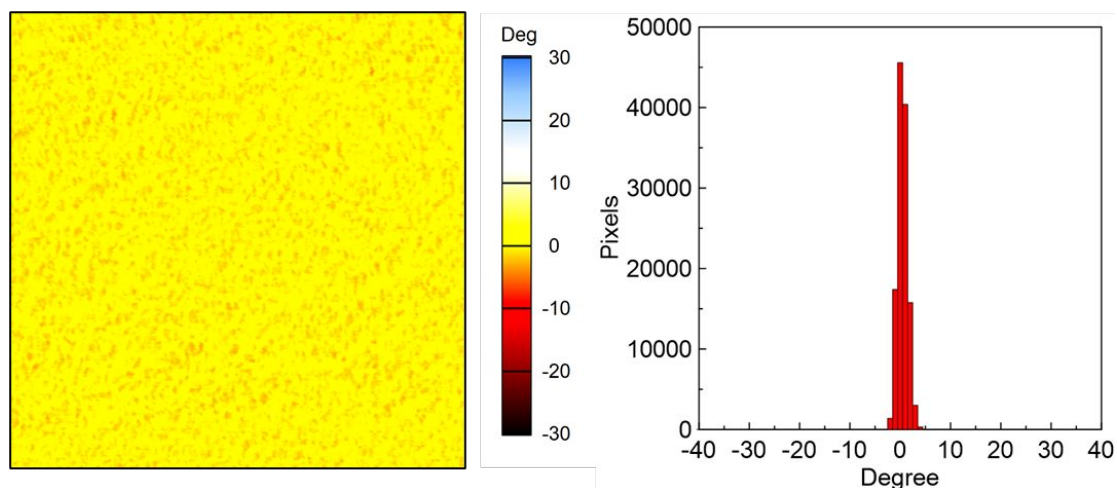
**Figure 2.** Normalized reaction rate as a function of acrylate group conversion for TTGDA (dashed line) systems modified with a) end-functionalized and b) random-functionalized prepolymers. All formulations were composed of 2:1 (w/w) TTGDA/Prepolymer with DMPA concentration of 0.5 wt %. Samples were photocured at 10 mW/cm<sup>2</sup> for 10 min.

### *Polymer Morphology*

Variations in photopolymerization kinetics typically indicate significant changes in network gelation, morphological development, and polymer properties.<sup>4,5,23,30</sup> The addition of different prepolymers into the TTGDA resin increases final double bond conversion and delays the time to reach the maximum rate. It is reasonable to believe that these changes in reaction kinetics indicate longer diffusion times for the TTGDA monomer and prepolymers prior to network gelation, significantly dictating the extent of phase separation during polymer formation. Previous work has shown that increasing the  $M_n$  of non-reactive prepolymers in dimethacrylate (e.g. TEGDMA) systems leads to observable phase separation due to overall reduction of system entropy, increasing Gibbs free energy of mixing and thus inducing greater thermodynamic instability during the course

of polymerization.<sup>31</sup> Consequently, we believe that the incorporation of OH-functionalized prepolymers with different architectures could also lead to different thermodynamic instabilities, tailoring nano/micro-structure formation during photopolymerization and with potentially different phase-separated domains.<sup>6,15,26</sup>

To investigate whether phase-separated domains are induced by adding end/random-functionalized prepolymers, atomic force microscopy (AFM) in tapping mode was used to examine polymer surface morphology and phase distribution. Tapping mode enables the cantilever tip to oscillate at a constant frequency. The existence of distinct phases with different local compositions and adhesion behavior will cause lower or higher delays in the tip oscillation depending on the inherent local properties of each phase. These delays in the tip oscillation are represented with variations in the phase angle.<sup>4,5</sup> Figure 3 shows the phase morphology and distribution for the neat TTGDA systems photocured at 10 mW/cm<sup>2</sup>. As expected, this system does not exhibit considerable phase contrast and the presence of small variations is due to structural heterogeneities, i.e. regions with high and low cross-linked densities, common for highly cross-linked networks.<sup>5</sup> In addition, further information regarding polymer surface morphology is obtained through phase distribution plots. These plots show the number of pixels that exhibit similar local phase behavior for a certain phase lag degree. Thus, only small deviations from the default oscillation indicate single-domain polymers while enhanced deviation shows formation of multiple domains. The phase distribution for the neat TTGDA system appears very narrow suggesting a single-domain.



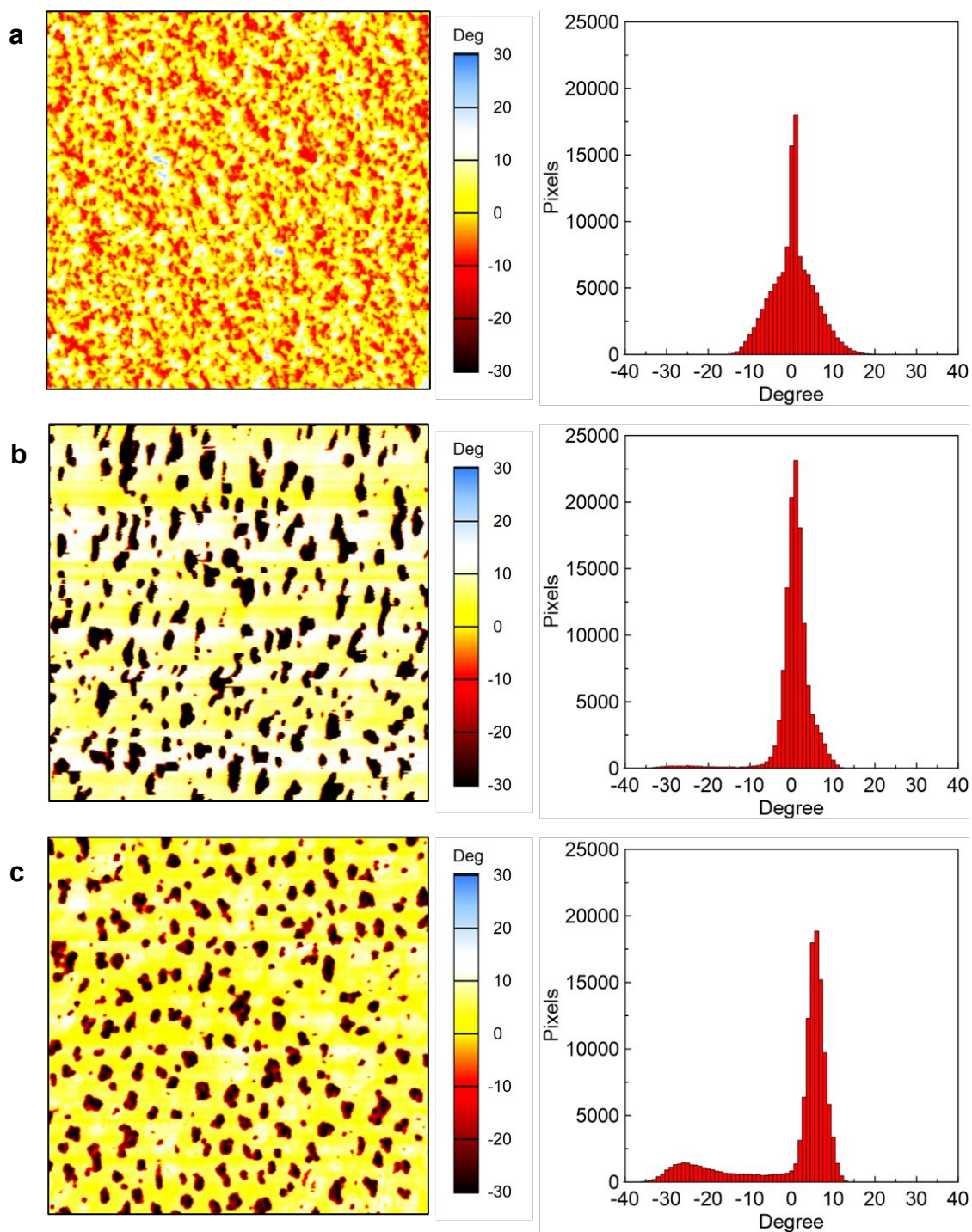
**Figure 3.** AFM phase image and distribution of a polymer system composed of neat TTGDA. The system was photopolymerized at  $10 \text{ mW/cm}^2$  for 10 min. The dimensions of the polymer surface area are  $1 \times 1 \text{ }\mu\text{m}$ . Photoinitiator DMPA concentration was 0.5 wt %.

Figure 4 shows polymer morphologies and phase distributions from AFM for photopolymerized systems modified with end-functionalized prepolymers. Specifically, well integrated but distinct phase-separated domains appear to form for the TTGDA/E15k system. In addition, TTGDA systems modified with E30k or E50k exhibit more distinct domains as indicated by the increased phase contrast due to increased prepolymer concentration in the systems which likely contributes to a greater degree of phase separation. Moreover, phase distributions become more dispersed with increasing prepolymer  $M_n$ . While E15k-modified systems exhibit evenly distributed phases with the short chain length of the linear domains, a second distinct domain appears to form by increasing prepolymer  $M_n$ . This behavior supports that E30k and E50k prepolymers tend to promote higher extent of phase separation likely due to higher degrees of self-association of prepolymers between the crosslinks. On the other hand, polymer morphologies and phase distributions appear much different for systems modified with random-functionalized prepolymers as shown in Figure 5. For



example, these systems exhibit significantly increased phase contrast compared to end-functionalized prepolymers. Even though increasing the  $M_n$  appears to induce more distinct domains due to thermodynamically-driven phase separation, the effect of increasing the  $M_n$  on phase distribution is not as significant as that of end-functionalized prepolymers. Additionally, all systems exhibit very broad phase distributions and observable peaks for both negative and positive phase angles. Interestingly, these peaks appear much lower than those for end-functionalized systems, indicating a larger transition from softer to harder domains. This overall behavior may be related to the random OH group position which likely forms more hydrogen bonds with the polymer network due to prepolymer ability to interact throughout acrylate networks, resulting in more intermixed domains.

Consequently, each prepolymer architecture has a different impact on network formation and phase separation during photopolymerization. It is reasonable to believe that end-functionalized prepolymers self-associate to a greater degree due to interchain hydrogen bonding between the OH groups as represented in Scheme 1. On the other hand, random-functionalized prepolymers may self-associate to a lesser degree because of their more hydrophilic character with the random distribution of HEA enabling greater proximity of OH groups to the acrylate network. Furthermore, both prepolymer types may also re-arrange/re-initiate during photopolymerization due to prepolymer synthesis using a RAFT agent. This RAFT re-initiation could form smaller domains since the prepolymer chain may break and re-connect during the cross-linking process.



**Figure 4.** AFM phase images and distributions of polymer systems with 2:1 (w/w) a) TTGDA/E15k, b) TTGDA/E30k, and c) TTGDA/E50k. Samples were photopolymerized at 10 mW/cm<sup>2</sup> for 10 min using 0.5 wt % DMPA. The dimensions of each polymer surface area are 1 x 1  $\mu$ m.

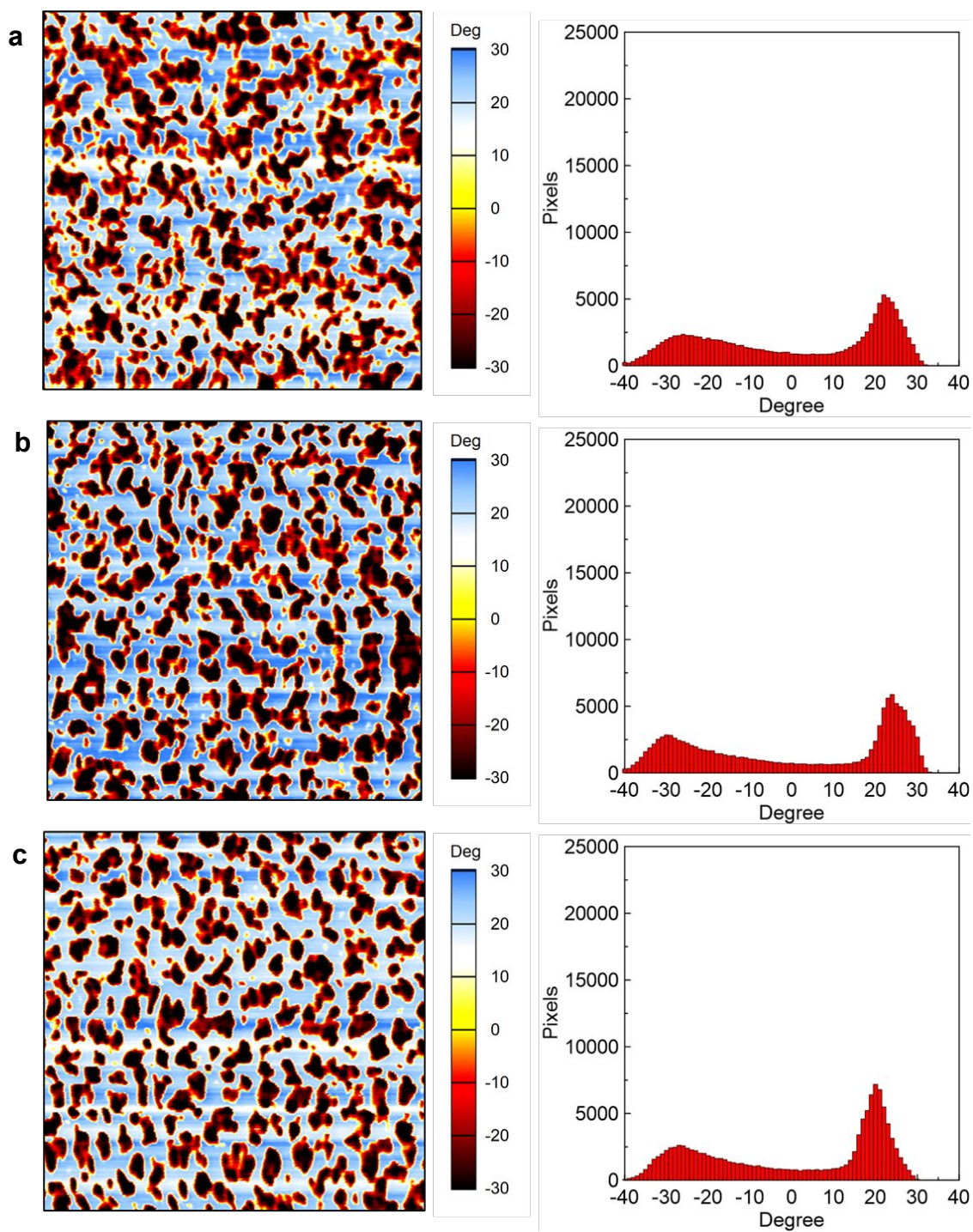
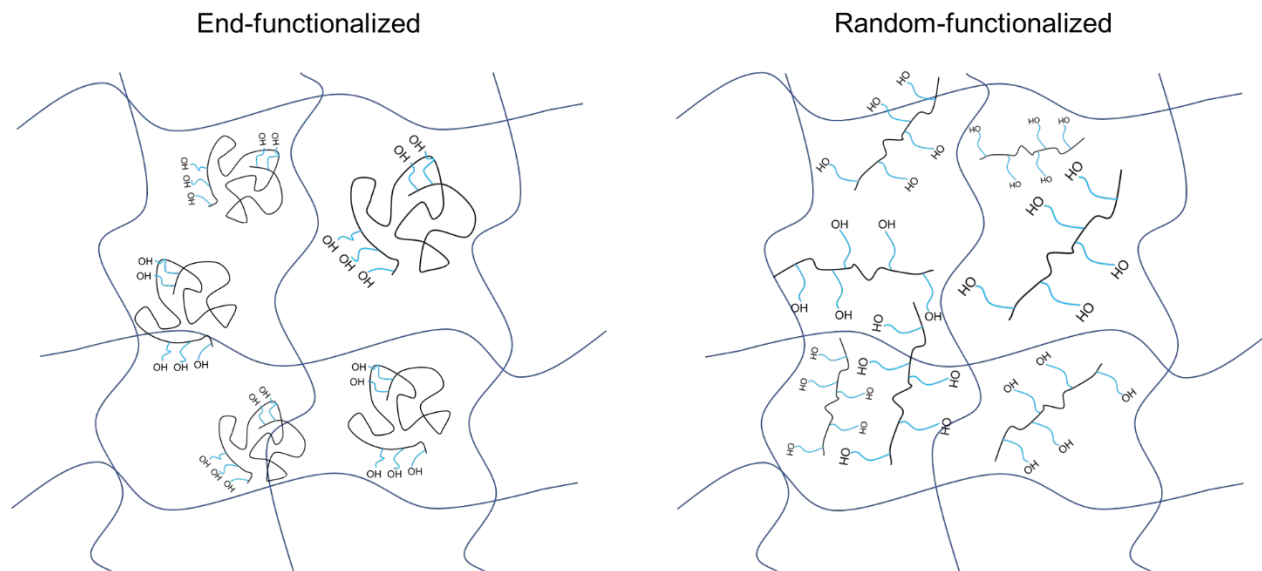


**Figure 5.** AFM phase images and distributions of polymer systems with 2:1 (w/w) a) TTGDA/R15k, b) TTGDA/R30k, and c) TTGDA/R50k. Samples were photopolymerized at 10 mW/cm<sup>2</sup> for 10 min using 0.5 wt % DMPA. The dimensions of each polymer surface area are 1 x 1  $\mu$ m.



**Scheme 1.** Representation of possible prepolymer rearrangements in the polymer networks.

### *Thermomechanical Properties*

The morphologies from AFM show that the formulation composition and prepolymer architecture can enable various phase-separated polymer morphologies. The formation of continuous and smaller hard/soft phase-separated domains has shown great promise in controlling glass transition temperature ( $T_g$ ) while enhancing Young's modulus and tensile toughness.<sup>4,5</sup> Therefore, it is reasonable to believe that the thermal and mechanical behavior of prepolymer-modified systems may also change due to formation of observable phase-separated domains with significant variations in phase distribution depending on  $M_n$  and OH placement.

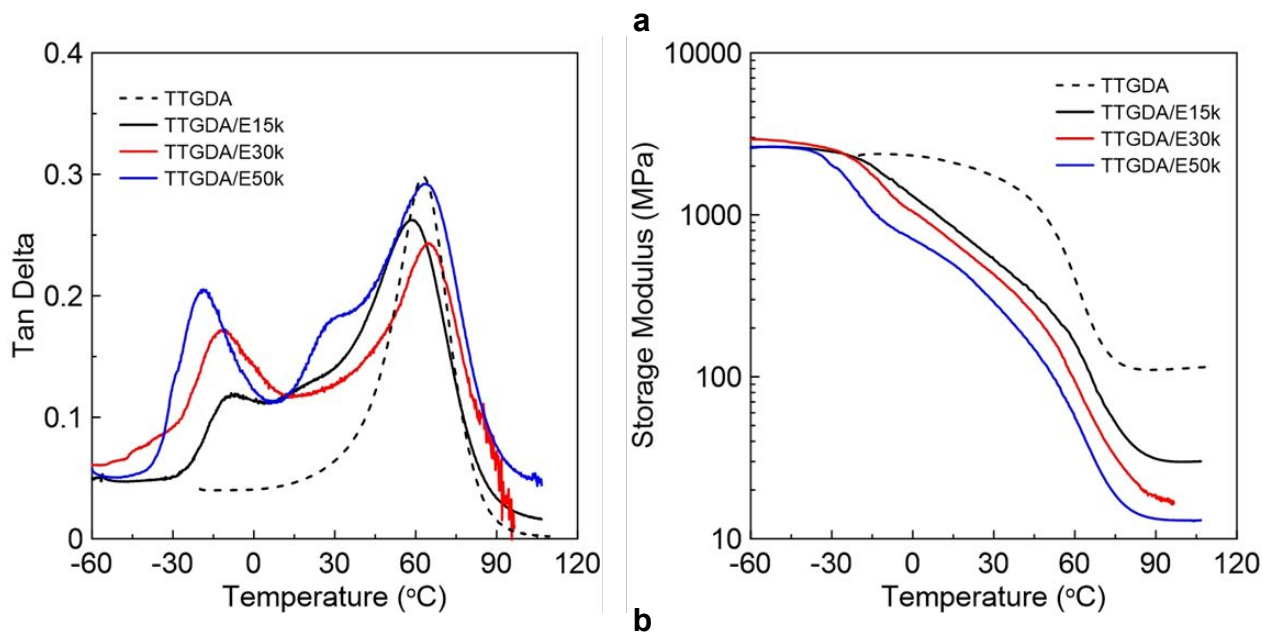
To understand the impact of polymer morphology on thermomechanical properties,  $\tan(\delta)$  behavior and storage modulus were investigated using dynamic mechanical analysis (DMA). Typically,  $\tan(\delta)$  peaks are associated with the  $T_g$  and can be used to assess the degree of phase separation, while storage modulus gives information regarding material elasticity and the ability

to store energy after undergoing a process.<sup>32,33</sup> Figure 6 shows the  $\tan(\delta)$  profiles and storage modulus for pure TTGDA and for systems modified with end and random-functionalized prepolymers. TTGDA systems exhibit a  $T_g$  at around 65 °C, as indicated by the single  $\tan(\delta)$  peak. Incorporating OH-functionalized prepolymers results in the formation of polymers with two  $\tan(\delta)$  peaks. A high temperature  $\tan(\delta)$  peak is observed at around 65 °C likely related to the TTGDA-rich domains and a low temperature  $\tan(\delta)$  peak appears between -15 and -25 °C depending on prepolymer type and concentration. This negative  $T_g$  can be associated with the prepolymer-rich domains since all prepolymers are synthesized with approximately 80 wt % BA as pure BA polymer exhibits a  $T_g$  of around -50 °C.<sup>34</sup> It is important to note that the small shoulder that appears at around 30 °C for TTGDA/E50k systems could be related to the formation of an intermediate phase region caused either by the network re-arrangement due to RAFT agent or due to significant self-association of this particular prepolymer, contributing to slightly different  $\tan(\delta)$  behavior than the other systems. The overall behavior also confirms the formation of polymers with phase-separated soft and hard domains as shown in AFM images. Additionally, the peak height of  $\tan(\delta)$  at lower temperatures increases with prepolymer  $M_n$  due to the higher concentration of both linear BA and HEA within the soft domain. These changes in  $\tan(\delta)$  behavior suggest that increasing prepolymer  $M_n$  or changing the OH group placement can significantly impact polymer structure and the degree of phase separation.

Furthermore, the introduction of prepolymers has a significant effect on storage modulus of TTGDA. For pure TTGDA systems, the modulus in the glassy region is almost constant up to temperatures of 10 °C, followed by a sharp drop at 60 °C. On the other hand, the modulus in the glassy region of prepolymer-modified systems remains flat only up to approximately -15 °C,



followed by a gradual decrease in modulus as the temperature increases. Additionally, the incorporation of prepolymers results in a significant reduction in the storage modulus of the rubbery plateau by one order of magnitude. While the storage modulus of the rubbery plateau decreases with increasing  $M_n$  of end-functionalized prepolymers, this trend does not seem to be the same for random-functionalized prepolymers which demonstrate similar values for any  $M_n$ . Again, this behavior could be due to enhanced self-association of the high  $M_n$  end-functionalized prepolymers which is very common in block type prepolymers.<sup>35</sup> In addition, the overall reduction in storage modulus indicates that the apparent cross-link density of these systems is much lower than that for neat TTGDA.



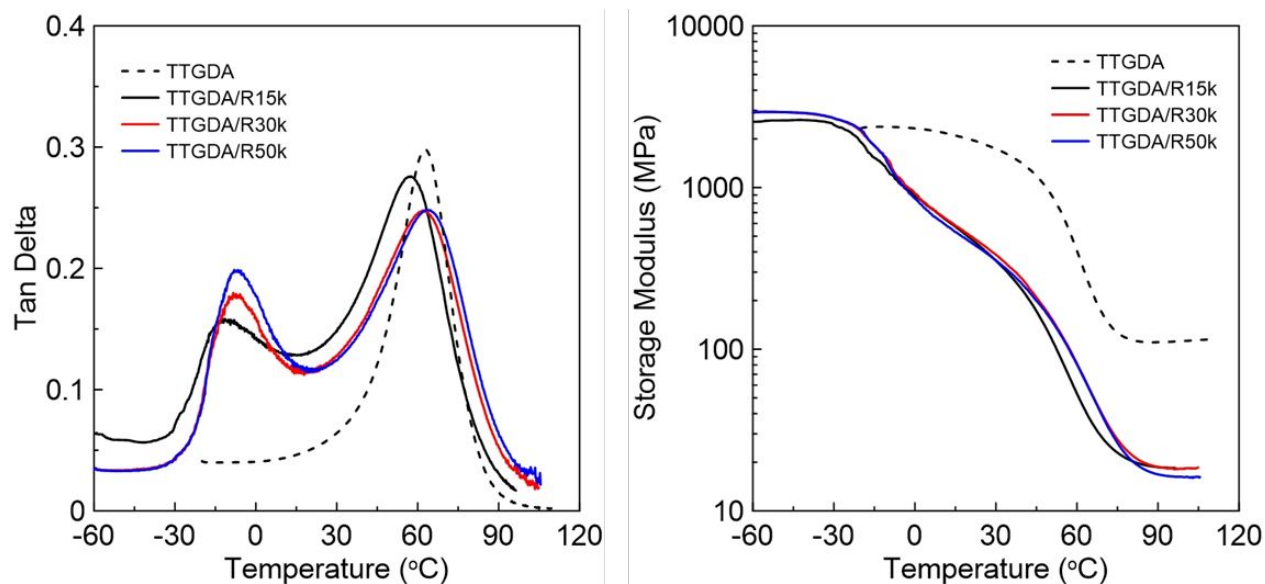


**Figure 6.** Tan( $\delta$ ) and storage modulus profiles as a function of temperature for TTGDA systems modified with a) end-functionalized OH groups and b) random-functionalized OH groups prepolymers. Samples are photopolymerized at 10 mW/cm<sup>2</sup> for 10 min using 0.5 wt % DMPA.

Based on the dramatic changes in tan( $\delta$ ) and storage modulus behaviors, as well as the formation of polymer networks with multiple  $T_g$ 's, it is reasonable to believe that each system will exhibit different mechanical properties. To investigate these potential changes in macroscopic properties, stress as a function of strain was evaluated using DMA. Figure 7 shows stress as a function of strain for TTGDA systems modified with different prepolymers. The pure TTGDA shows the highest Young's modulus with a very low elongation at break of approximately 5%. This stress-strain behavior is related to the high cross-link density and the formation of a single-domain network with high  $T_g$ . Incorporating E15k or E30k into the TTGDA system results in a considerable increase in elongation at break of up to 6 times and a slight decrease in Young's modulus. For TTGDA/E50k systems, elongation at break increases by a factor of 2 compared to the neat TTGDA with further decrease in Young's modulus. On the other hand, random-

functionalized prepolymers exhibit a more significant increase in elongation at break compared to that for end-functionalized systems. In this case, the addition of R15k or R30k increases elongation at break by roughly 9 times. When incorporating the prepolymer with the highest  $M_n$  (R50k), the elongation at break appears again to decrease compared to systems with lower  $M_n$  prepolymers, but still nearly 5 times higher than that of pure TTGDA. Moreover, Young's modulus is reduced compared to TTGDA, but maintains similar values for all random-functionalized prepolymer systems.

The mechanical behavior of systems modified with OH-functionalized prepolymers is likely related to formation of phase-separated soft/hard domains, with the high  $T_g$  cross-linked domains resisting the initial stress and the low  $T_g$  linear domains providing the necessary network flexibility that enables additional stretch. However, the formation of more distinct phase-separated domains for systems modified with either E50k or R50k has a detrimental effect on elongation at break with reduced values. These decreases may be due to fewer interactions between the soft prepolymers and hard acrylate network, likely imparted from different degrees of self-association of each prepolymer. It is also worth mentioning that relatively large viscous prepolymers tend to have low or no mobility during photocuring, resulting in lower degrees of interfacial interaction and hydrogen bonding between the compositionally different domains. Additionally, these prepolymers significantly reduce overall cross-link density which can account for the decreased Young's modulus.



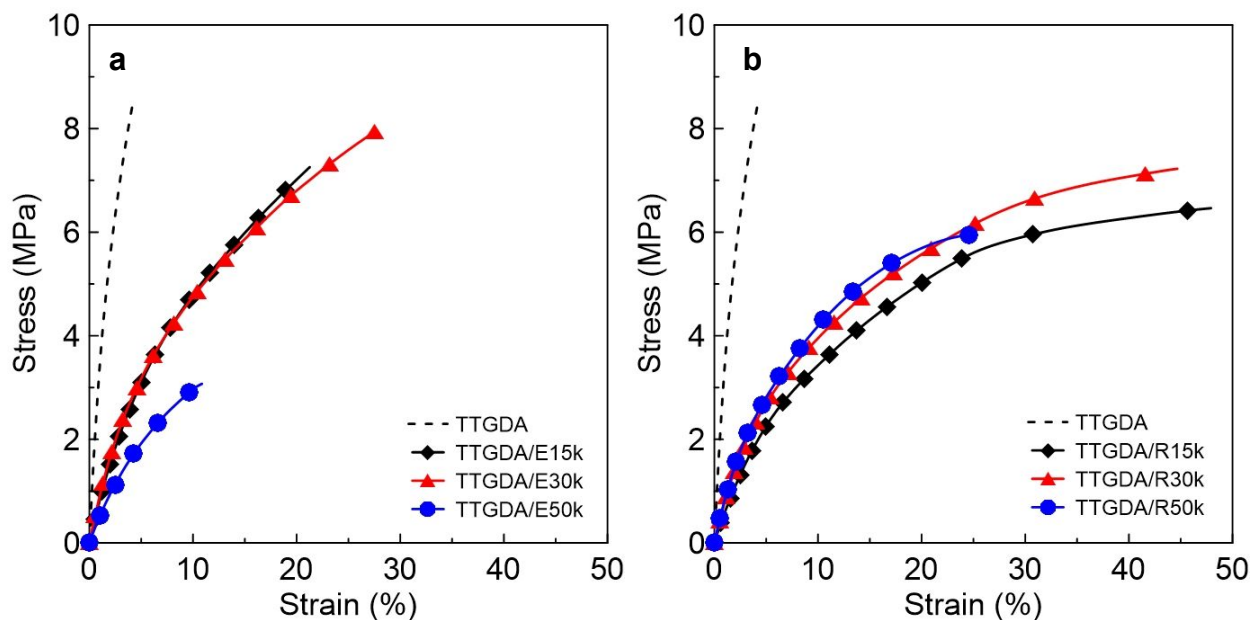


**Figure 7.** Stress as a function of strain for TTGDA systems modified with a) end-functionalized and b) random-functionalized prepolymers. Samples are photopolymerized at 10 mW/cm<sup>2</sup> for 10 min using 0.5 wt % DMPA.

Because of the significant changes in stress and strain behavior imparted from the prepolymer addition into TTGDA formulation, these materials should exhibit variations on the amount of absorbed energy before breaking. Prior work has shown that changes in the cross-linking processes for radical/cationic systems resulted in different interactions between the soft and hard domains, leading to enhanced elongation at break, a twofold increase in maximum stress, and significant improvement of tensile toughness and impact strength.<sup>5</sup> In this work, the incorporation of prepolymers into the TTGDA system enhances network flexibility and elongation at break, impacts cross-link density, and forms nano/micro-structured polymers with multiple  $T_g$ 's and different phase distributions. Based on these morphological and thermomechanical changes, the prepolymer-modified polymers should exhibit enhanced energy absorbance (i.e. toughness) before breaking. Figure 8 shows polymer toughness for TTGDA systems modified with end/random-

functionalized prepolymers as calculated from the area under stress-strain curves at 20 °C. The pure TTGDA system demonstrates a relatively low toughness of nearly 0.25 MJ/m<sup>3</sup> likely due to network brittleness and inconsistency in cross-link density. As compared to the TTGDA system, polymer toughness demonstrates a 4-fold and 8-fold increase when incorporating E15k and E30k, respectively. End-functionalized prepolymers of higher M<sub>n</sub> (E50k) exhibit similar toughness with pure TTGDA. As for systems modified with random-functionalized prepolymers, toughness increases by approximately 9 and 8 times for TTGDA/R15k and TTGDA/R30k systems, respectively. Additionally, the incorporation of R50k leads to a nearly 5-fold increase in toughness.

This significant increase in toughness for TTGDA systems modified with end/random-functionalized prepolymers (with notable exception of E50k) may be due to the presence of well dispersed linear/soft domains within the cross-linked TTGDA domains. As crack propagation forces develop throughout the polymer network, the presence of prepolymer-rich domains prevents further expansion and enhances thermal dissipation. Additionally, it can be assumed that most of the prepolymer-modified systems exhibit enhanced toughness due to intermolecular hydrogen bonding between the hydrogen and the strongly electronegative oxygen in the ether and ester groups of TTGDA. The hydroxyl groups can form many types of hydrogen bonds including those between hydroxyl groups as well as between hydroxyl and carbonyl groups with a strength on the order of about 20 kJ/mol.<sup>27</sup> This high energy and the formation of different domain distributions via photo-induced phase separation significantly mitigate the propagation of cracks. Although hydrogen bonding and domain flexibility help to enhance mechanical behavior, the incorporation of E50k prepolymer does not increase TTGDA toughness likely due to significantly decreased cross-link density and reduced interactions between prepolymers and polymer network.

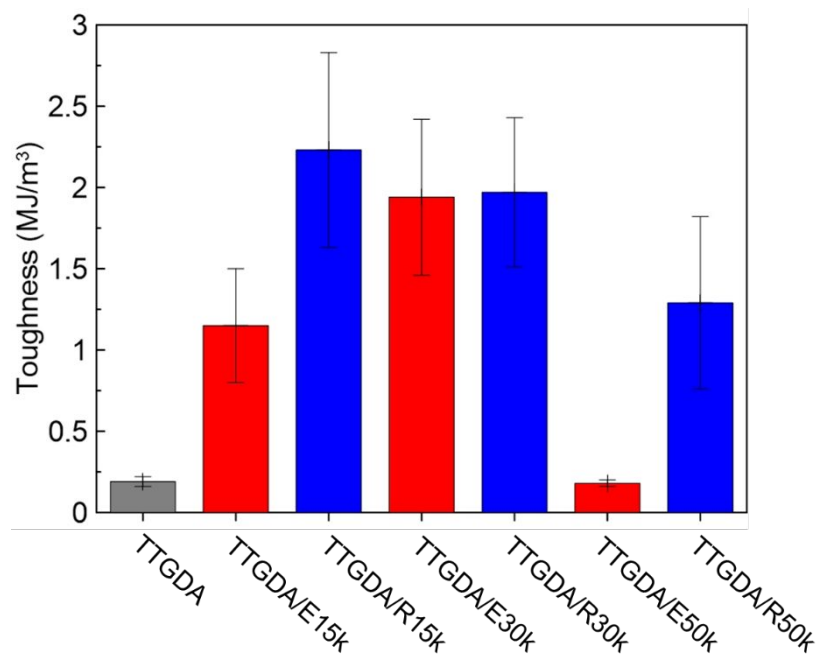


**Figure 8.** Tensile toughness for a system with neat TTGDA (dark grey), and for systems modified with end-functionalized (red) and random-functionalized (blue) prepolymers. Samples are photopolymerized at 10 mW/cm<sup>2</sup> for 10 min using 0.5 wt % DMPA. Each experiment was conducted 4 times with the error bars representing standard deviation.

Given the evidence that phase-separated polymers contain both rubbery and glassy regions with different phase distributions, toughness might significantly change over a wide range of temperature due to variations of chain mobility as well as the differences in  $\tan(\delta)$  and storage modulus. To probe any changes in the absorbed energy of single and multi-phase systems, polymer toughness was investigated at different temperatures (0, 20, 50, and 80 °C). These temperatures were selected to examine the behavior of these systems at conditions close to the lower of two primary  $T_g$ 's, between the two  $T_g$ 's, and above the higher  $T_g$  and to show the performance of phase-separated polymers under dramatic changes in environmental conditions. Figure 9 shows

toughness for neat TTGDA and TTGDA/R15k systems at these different temperatures. R15k prepolymer systems were chosen because they exhibit the greatest toughness enhancement as shown in Figure 8. Toughness of the neat TTGDA systems demonstrates small variations with the highest values observed at 20 and 50 °C. When adding R15k, toughness is significantly higher at all specific temperature compared to that of TTGDA. For example, an increase of about 11-fold and 9-fold can be observed at the lowest and room temperatures, respectively. Additionally, a smaller but still important increase in toughness by a factor 5 is observed at 50 and 80 °C compared to that of the corresponding neat TTGDA. Thus, these phase-separated polymers can absorb the greatest amount of energy before breaking when stress is applied at environmental conditions that fall between the first and second  $\tan(\delta)$  peaks (Figure 6). This behavior can be attributed to the network flexibility imparted from the addition of the linear prepolymers, the enhanced prepolymer chain mobility, and the presence of phase-separated polymers with multiple  $T_g$ 's which enables multiple glassy and rubbery regions to co-exist at the same network. On the other hand, pure TTGDA systems are very brittle over the examined temperatures with low network mobility, leading to insufficient energy absorbance.

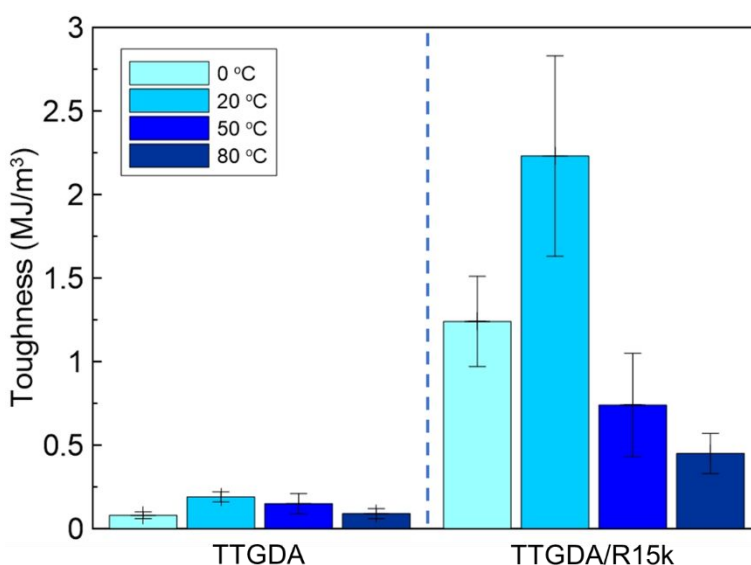


**Figure 9.** Polymer toughness of systems with neat TTGDA and 2:1 (w/w) TTGDA/R15k at different temperatures. Samples are photopolymerized at 10 mW/cm<sup>2</sup> for 10 min using 0.5 wt % DMPA. Each experiment was conducted 4 times with the error bars representing standard deviation.

### *Impact Strength of 3D Printed Objects*

The addition of OH-functionalized prepolymers into the TTGDA resin enables fabrication of unique polymer morphologies, leading to enhanced toughness. To further understand the mechanical/fracture properties of systems composed of PR48 resin and different prepolymers, the impact strength of 3D printed objects was investigated using Izod impact testing. Impact strength is a more direct measure of material energy absorption before fracture which shows the ability of materials to resist a sudden impact.<sup>36</sup> Previous work has shown that the addition of silicon-modified polyurethane prepolymers into a brittle epoxy resin resulted in a 5-fold increase in impact strength due to network flexibility imparted from improved entanglements between prepolymers and cross-linked domains.<sup>37</sup> Therefore, the incorporation of custom-synthesized prepolymers could also affect the performance of a highly cross-linked/brittle formulation such as PR48.

Figure 10 shows the impact strength of PR48 systems modified with different OH-functionalized prepolymers and CN9002 oligomer. CN9002 is a proprietary difunctional aliphatic urethane acrylate oligomer that imparts significant flexibility and film forming properties.<sup>38</sup> Similar to the prepolymers studied herein, CN9002 contributes to hydrogen bonding through the urethane CNH groups in resin formulations. In addition, this urethane diacrylate can react with the TTGDA monomer during photopolymerization and become part of the polymer network. It is important to

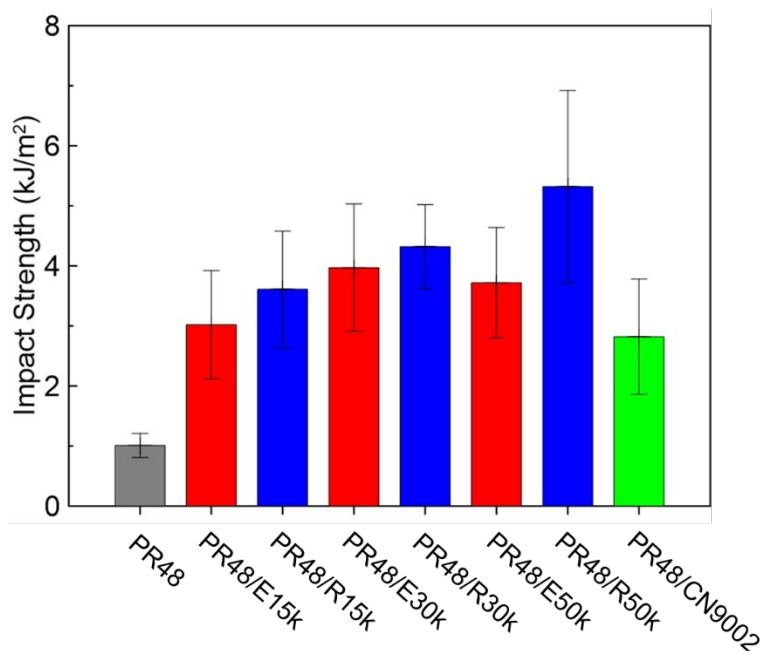
note that all 3D printed objects were UV post-cured at  $20 \text{ mW/cm}^2$  for 10 min using a 405 nm LED lamp in order to ensure complete polymerization of the remaining carbon-carbon double bonds. Photos of representative 3D printed parts are shown in the supplementary section where PR48 is very clear, while PR48/prepolymer systems appear less transparent likely due to some degree of phase separation (Figure S1). Moreover, PR48 systems modified with OH-functionalized prepolymers exhibit yellowness due to the RAFT agent used in the synthesis.

Figure 10 shows an impact strength of approximately  $1 \text{ kJ/m}^2$  for the control PR48 resin which is significantly lower than that of PR48/prepolymer systems. This relatively low resistance to a sudden force could be related to the formation of brittle/highly-crosslinked polymeric materials. Incorporation of prepolymers into the PR48 results in a significant increase in impact strength. For example, the addition of E15k increases impact strength by 200% while the E30k prepolymer enables a 300% increase. For E50k-modified systems, impact strength appears to slightly decrease compared to the prepolymers with lower  $M_n$ . These higher impact strength values could be partly related to the phase-separated structures which can better dissipate stress propagation throughout the polymer network and partly to enhanced hydrogen bonding, especially for E15k and E30k prepolymers that likely do not self-associate to the same extent as E50k prepolymer. On the other hand, the addition of random-functionalized prepolymers exhibits slightly different behavior. In this case, all prepolymers appear to increase gradually the impact strength with increasing  $M_n$ . Specifically, impact strength increases by 250%, 350%, and 450% when mixing PR48 with R15k, R30k, and R50k prepolymers, respectively. These results may be due to limited self-association of random-functionalized prepolymers and their ability to be well-dispersed as shown in Figure 5. In

addition, these prepolymers likely result in greater physical entanglements and hydrogen bonding interactions with the polymer network.

Interestingly, incorporating CN9002 increases impact strength of PR48 by almost 200%. The impact strength of about 2.8 kJ/m<sup>2</sup> of PR48/CN9002 system not only is lower than those of all systems modified with OH-functionalized prepolymers but also is only half the value from the PR48/R50k system. This more remarkable increase in impact strength for systems with custom-synthesized prepolymers may be associated with the formation of phase-separated and well-dispersed soft/hard domains in the polymer network as indicated by the multiple tan( $\delta$ ) peaks shown in Figure S2. In addition, the OH groups likely form various hydrogen bonds which enhances intermolecular strength and interlayer adhesion.

These results validate our hypothesis that incorporation of linear prepolymers with different  $M_n$  and OH group placements can significantly alter polymer morphology and properties. Using photo-induced phase separation helps to fabricate polymer morphologies with various domain distributions and hydrogen bonding interactions, leading to highly cross-linked but flexible polymer networks with improved toughness and impact strength.



**Figure 10.** Impact strength for PR48 (grey) systems modified with end-functionalized (red), random-functionalized (blue) prepolymers and CN9002 (green) oligomer. All photocurable systems are prepared with a 4:1 (w/w) PR48/prepolymer ratio. Each layer of all 3D printed objects was photopolymerized at approximately 20 mW/cm<sup>2</sup> using a 405 nm LED light source imparted in the Autodesk Ember 3D printer. The error bars represent the standard deviation of 5 experiments.

## Conclusion

This study shows that OH-functionalized prepolymers can be used to form separate soft domains within glassy highly cross-linked acrylate systems, generating polymers with controlled thermo-mechanical properties. The OH group placement and prepolymer  $M_n$  play an important role in the degree of phase separation and domain distribution. Tan( $\delta$ ) profiles reveal that increasing the  $M_n$  results in more distinct phase-separated domains, as indicated by the prepolymer-rich tan( $\delta$ ) peak height, which is more distinct for the end-functionalized prepolymers due to self-association. The



random-functionalized prepolymers appear to interact to a greater degree with the acrylate network during photopolymerization, leading to more diverse/intermixed domains. These interactions between the acrylate networks and prepolymer domains enable significant enhancement of elongation at break, especially for random-functionalized prepolymers due to better hydroxyl group distribution and thus hydrogen bonding between prepolymers and the polymer network. This behavior contributes to significantly improved toughness at a range of temperatures. In addition, including OH-functionalized prepolymers in a model acrylate formulation significantly improves the impact strength of 3D printed parts more than 5-fold and almost double that observed with a commercial CN9002 oligomer system. Our work shows that controlling the architecture of OH-functionalized prepolymers can impact the domain distribution of phase-separated morphologies, resulting in much tougher polymers that can be used for a range of applications including 3D printing.

## **Conflict of Interest**

There are no conflicts of interest to declare.

## **Acknowledgements**

The authors acknowledge the financial support of this research from the Industry/University Cooperative Research Center (IUCRC) for Fundamentals and Applications of Photopolymerizations and the National Science Foundation (CBET-1438486).

## **Supporting Information**

Representative images and  $\tan(\delta)$  behavior of 3D printed objects composed of PR48 formulations modified with different OH-functionalized prepolymers or CN9002 oligomer.

## References

- (1) Ligon-Auer, S. C.; Schwentenwein, M.; Gorsche, C.; Stampfl, J.; Liska, R. Toughening of Photo-Curable Polymer Networks: A Review. *Polym. Chem.* **2016**, *7* (2), 257–286.
- (2) Schulze, M. W.; McIntosh, L. D.; Hillmyer, M. A.; Lodge, T. P. High-Modulus, High-Conductivity Nanostructured Polymer Electrolyte Membranes via Polymerization-Induced Phase Separation. **2014**.
- (3) Szczepanski, C. R.; Darmanin, T.; Guittard, F. Spontaneous, Phase-Separation Induced Surface Roughness: A New Method to Design Parahydrophobic Polymer Coatings with Rose Petal-like Morphology. *ACS Appl. Mater. Interfaces* **2016**, *8* (5), 3063–3071.
- (4) Hasa, E.; Scholte, J. P.; Jessop, J. L. P.; Stansbury, J. W.; Guymon, C. A. Kinetically Controlled Photoinduced Phase Separation for Hybrid Radical/Cationic Systems. *Macromolecules* **2019**, *52* (8), 2975–2986.
- (5) Hasa, E., Stansbury, J. W., & Guymon, C. A. Manipulation of crosslinking in photo-induced phase separated polymers to control morphology and thermo-mechanical properties. *Polymer*, **2020**, 202.
- (6) Scholte, J. P.; Ki Kim, S.; Lester, C. L.; Guymon, C. A. Effects of Directed Architecture in Epoxy Functionalized Prepolymers for Photocurable Thin Films. *J. Polym. Sci. Part A*

- Polym. Chem.* **2017**, *55* (1), 144–154.
- (7) Siddhamalli, S. K.; Kyu, T. Toughening of Thermoset / Thermoplastic Composites Via Reaction-Induced Phase Separation : Epoxy / Phenoxy Blends. *J. Appl. Polym. Sci.* **2000**, *77* (April), 1257–1268.
- (8) Bhattacharya, M. Polymer Nanocomposites-A Comparison between Carbon Nanotubes, Graphene, and Clay as Nanofillers. *Materials.* **2016**, *9* (4), 1–35.
- (9) Jordan, J.; Jacob, K. I.; Tannenbaum, R.; Sharaf, M. A.; Jasiuk, I. Experimental Trends in Polymer Nanocomposites - A Review. *Mater. Sci. Eng. A* **2005**, *393* (1–2), 1–11.
- (10) Martin-Gallego, M.; Verdejo, R.; Lopez-Manchado, M. A.; Sangermano, M. Epoxy-Graphene UV-Cured Nanocomposites. *Polymer.* **2011**, *52* (21), 4664–4669.
- (11) Liu, Y. Polymerization-Induced Phase Separation and Resulting Thermomechanical Properties of Thermosetting/Reactive Nonlinear Polymer Blends: A Review. *J. Appl. Polym. Sci.* **2013**, *127* (5), 3279–3292.
- (12) Crawford, K. E.; Sita, L. R. De Novo Design of a New Class of “Hard-Soft” Amorphous, Microphase-Separated, Polyolefin Block Copolymer Thermoplastic Elastomers. *ACS Macro Lett.* **2015**, *4* (9), 921–925.
- (13) Guo, Y.; Gao, X.; Luo, Y. Mechanical Properties of Gradient Copolymers of Styrene and N-Butyl Acrylate. *J. Polym. Sci. Part B Polym. Phys.* **2015**, *53* (12), 860–868.
- (14) Kayaman-Apohan, N.; Amanoel, A.; Arsu, N.; Güngör, A. Synthesis and Characterization of UV-Curable Vinyl Ether Functionalized Urethane Oligomers. *Prog. Org. Coatings* **2004**, *49* (1), 23–32.

- (15) Szczepanski, C. R.; Pfeifer, C. S.; Stansbury, J. W. A New Approach to Network Heterogeneity: Polymerization Induced Phase Separation in Photo-Initiated, Free-Radical Methacrylic Systems. *Polymer*. **2012**, *53* (21), 4694–4701.
- (16) Szczepanski, C. R.; Stansbury, J. W. Modification of Linear Prepolymers to Tailor Heterogeneous Network Formation through Photo-Initiated Polymerization-Induced Phase Separation. *Polymer*. **2015**, *70*, 8–18.
- (17) Scholte, J. Effects of Prepolymer Structure on Photopolymer Network Formation and Thermomechanical Properties, University of Iowa, 2017.
- (18) Autodesk. Autodesk Standard Clear Prototyping Resin (PR48). **2015**, 48.
- (19) Keddie, D. J. A Guide to the Synthesis of Block Copolymers Using Reversible-Addition Fragmentation Chain Transfer (RAFT) Polymerization. *Chem. Soc. Rev.* **2014**, *43* (2), 496–505.
- (20) Fenoli, C. R.; Wydra, J. W.; Bowman, C. N. Controllable Reversible Addition-Fragmentation Termination Monomers for Advances in Photochemically Controlled Covalent Adaptable Networks. *Macromolecules* **2014**, *47* (3), 907–915.
- (21) Green, B. J.; Guymon, C. A. Modification of Mechanical Properties and Resolution of Printed Stereolithographic Objects through RAFT Agent Incorporation. *Addit. Manuf.* **2019**, *27*, 20–31.
- (22) DePierro, M. A.; Baguenard, C.; Allan Guymon, C. Radical Polymerization Behavior and Molecular Weight Development of Homologous Monoacrylate Monomers in Lyotropic

- Liquid Crystal Phases. *J. Polym. Sci. Part A Polym. Chem.* **2016**, *54* (1), 144–154.
- (23) Bowman, C. N.; Kloxin, C. J. Toward an Enhanced Understanding and Implementation of Photopolymerization Reactions. *AIChE J.* **2008**, *54* (11), 2775–2795.
- (24) Chatani, S.; Kloxin, C. J.; Bowman, C. N. The Power of Light in Polymer Science: Photochemical Processes to Manipulate Polymer Formation, Structure, and Properties. *Polym. Chem.* **2014**, *5* (7), 2187–2201.
- (25) Kloosterboer, J. G. Network Formation by Chain Crosslinking Photopolymerization and Its Applications in Electronics. In *Electronic Applications*; Springer Berlin Heidelberg: Berlin, Heidelberg, 1988; pp 1–61.
- (26) Szczepanski, C. R.; Stansbury, J. W. Accessing Photo-Based Morphological Control in Phase-Separated, Cross-Linked Networks through Delayed Gelation. *Eur. Polym. J.* **2015**, *67*, 314–325.
- (27) Lee, T. Y.; Roper, T. M.; Jönsson, E. S.; Guymon, C. A.; Hoyle, C. E. Influence of Hydrogen Bonding on Photopolymerization Rate of Hydroxyalkyl Acrylates. *Macromolecules* **2004**, *37* (10), 3659–3665.
- (28) Beuermann, S. Impact of Hydrogen Bonding on Propagation Kinetics in Butyl Methacrylate Radical Polymerizations. *Macromolecules* **2004**, *37* (3), 1037–1041.
- (29) Jansen, J. F. G. A.; Dias, A. A.; Dorsch, M.; Coussens, B. Fast Monomers: Factors Affecting the Inherent Reactivity of Acrylate Monomers in Photoinitiated Acrylate Polymerization. *Macromolecules* **2003**, *36* (11), 3861–3873.
- (30) Szczepanski, C. R. Design of Heterogeneous Network Structures Through Polymerization

Induced Phase Separation, University of Colorado, 2014.

- (31) Szczepanski, C. R.; Stansbury, J. W. Modification of Linear Prepolymers to Tailor Heterogeneous Network Formation through Photo-Initiated Polymerization-Induced Phase Separation. *Polymer*. **2015**, *70*, 8–18.
- (32) Menard, K. P. *DYNAMIC MECHANICAL ANALYSIS A Practical Introduction*; 1999.
- (33) Lipatov, Y. S. Interfacial Regions in the Phase-Separated Interpenetrating Networks. *Polym. Bull.* **2007**, *58* (1), 105–118.
- (34) Fernandez-Garcia, M.; Cuervo-Rodriguez, R.; Madruga, E. L. Glass Transition Temperatures of Butyl Acrylate-Methyl Methacrylate Copolymers. *J. Polym. Sci. Part B Polym. Phys.* **1999**, *37* (17), 2512–2520.
- (35) Asada, M.; Oshita, S.; Morishita, Y.; Nakashima, Y.; Kunimitsu, Y.; Kishi, H. Effect of Miscible PMMA Chain Length on Disordered Morphologies in Epoxy/PMMA-b-PnBA-b-PMMA Blends by in Situ Simultaneous SAXS/DSC. *Polymer*. **2016**, *105*, 172–179.
- (36) Campo, E. A. 2 - Mechanical Properties of Polymeric Materials. In *Selection of Polymeric Materials*; Campo, E. A., Ed.; Plastics Design Library; William Andrew Publishing: Norwich, NY, 2008; pp 41–101.
- (37) Bhuniya, S.; Adhikari, B. Toughening of Epoxy Resins by Hydroxy-Terminated, Silicon-Modified Polyurethane Oligomers. *J. Appl. Polym. Sci.* **2003**, *90* (6), 1497–1506.
- (38) Arkema Sartomer, [https://americas.sartomer.com/en/product-finders/product/f/sartomer\\_Urethane\\_US/p/cn9002/](https://americas.sartomer.com/en/product-finders/product/f/sartomer_Urethane_US/p/cn9002/) (accessed April 2022).